
SMART FAULT DETECTION IN NANOSATELLITE ELECTRICAL POWER SYSTEM

Alireza Rezaee

Department of Mechatronics, School of Intelligent Systems
 College of Interdisciplinary Science and Technology
 University of Tehran
 Tehran, Iran
 arrezaee@ut.ac.ir

Niloofar Nobahari

Department of Mechatronics, School of Intelligent Systems
 College of Interdisciplinary Science and Technology
 University of Tehran
 Tehran, Iran
 nobahari.niloofar@ut.ac.ir

Amin Asgarifar

Faculty of New Sciences and Technologies
 University of Tehran, Tehran, Iran

Farshid Hajati

School of Science and Technology
 Faculty of Science, Agriculture, Business and Law
 University of New England
 Armidale, NSW 2350, Australia
 fhajati@une.edu.au

January 5, 2026

ABSTRACT

This paper presents a new detection method of faults at Nanosatellites' electrical power without an Attitude Determination Control Subsystem (ADCS) at the LEO orbit. Each part of this system is at risk of fault due to pressure tolerance, launcher pressure, and environmental circumstances. Common faults are line to line fault and open circuit for the photovoltaic subsystem, short circuit and open circuit IGBT at DC to DC converter, and regulator fault of the ground battery. The system is simulated without fault based on a neural network using solar radiation and solar panel's surface temperature as input data and current and load as outputs. Finally, using the neural network classifier, different faults are diagnosed by pattern and type of fault. For fault classification, other machine learning methods are also used, such as PCA classification, decision tree, and KNN.

Keywords: fault diagnosis, machine learning, nanosatellite, electrical power system

1 Introduction

Nanosatellites, according to their missions, have several subsystems. The power subsystem generates, manages, and distributes power. The power subsystem is essential in all satellites. According to the mission type and requirements, this subsystem includes parts like photovoltaic solar arrays for converting the sun's energy and generating electrical power, DC to DC Maximum Power Point Tracker (MPPT) converter and regulator for power optimization and regulation. DC charge manager subsystem, loads, and switch mechanism are designed and implemented for a specific purpose [1].

The power generated by the photovoltaic solar array and the whole system is affected by the orbital condition and satellite circumstances such as orbital high, inclination, radiant intensity, heat flux, or radiation at orbit temperature that should be analyzed [2]. When the whole system and components work correctly, the satellite is able to carry on the mission. However, several faults may occur due to the launcher's shock and pressure. If these faults do not be detected at the right time, they may cause the whole system or mission failure.

1.1 Related Work

Beyond satellite power systems, related work on pattern recognition, control, and applied machine learning in power, biomedical, and telecommunication domains provides additional methodological support and motivation for our approach [22–59]. Research has been conducted on detecting, classifying, and diagnosing electrical equipment faults at the satellite power subsystem. Zhao et al. [3] proposed a method to detect faults at photovoltaic solar arrays based on Graph-Based Semi-Supervised Learning (GBSL). By GBSL, they detected faults that an Overcurrent Protection Device (OCPD) could not uncover. Zhao et al. [4] detected and diagnosed the photovoltaic solar systems' faults using a decision tree. Mohamed et al. [5] also detected photovoltaic solar systems' faults by neural networks and the genetic algorithm. In a converter proposed in [6], there was a method for detecting faults, detecting open circuit power switch faults without using additional hardware, and using the correct control loop in the PWM converter.

In aerospace projects, fault in Li-Ion battery is applied [7] because the density of energy is high and does with methods like diagnosis and distinguish fault based on Kalman Sequential Adaptive filter for looking state charge and DE charge of the battery, rate of charge, and de charge, estimate of state charge and DE charge (SOC), and health state (RUH) with use by back up vector machine and collect load information that is connected to it [8, 9].

The above-mentioned researches do not consider the fault diagnosis of the whole satellite's power system. Only two studies have discussed the fault diagnosis in the satellite's power subsystem. In the first research, the fault diagnosis and tolerance have been discussed based on the PCA method for any voltage, current, and temperature faults at sensors. This paper is only concerned about the accumulative fault on the power system's sensors [10]. In [11], each fault probabilities in the satellite's power system with Bayesian network is defined by knowledge of scientist but for using the Bayesian category without the use of scientist knowledge, fault probabilities must be determined or can be estimated by Gaussian equation [12].

In this paper, the faults of the whole power system, including photovoltaic parts, the DC to DC converter, and the battery are diagnosed and resolved. This paper separate faults using a detective method.

2 Materials and Methods

Satellite electrical power system consists of analog and digital circuits that include transistors, trustors, diodes, amplifiers, logic elements, switches, and connections. These parts are manufactured with specific reliabilities. The faulting rate in a component (λ) is defined as

$$\lambda = \frac{N_{\text{faulty}}}{N_{\text{total}} \times t}$$

where t is the outfit time hour unit (h), N_{faulty} is the number of faulty elements, and N_{total} is the total number of elements. This rate depends on temperature and the mode of operation. Table 1 lists the faulting rate in various components.

Table 1: Fault rate at temperature 40 °C for various components [13, 14].

Equipment	$\lambda (10^{-9}/\text{h})$
Transistor	10–9
Trustor (power switch family)	10–9
Digital integrated circuit	30
Logical elements	30
Analog switches	2000
Amplifier	10–9
Diode	10–9
Battery Li-Ion	10–9
Solar array	10–9

Using the faulting rate, we can diagnose faults at electrical power system components such as IGBTs, MPPT converters and regulators, solar array, and battery. Open circuit and line-to-line faults in solar array, short circuit and open circuit faults in IGBTs, MPPT converters and regulators, and ground fault in battery are feasible in nanosatellite power systems.

Figure 1 shows the overall block diagram of the proposed fault diagnosis model. First of all, the system must be recognized by virtual neural network for detecting and classify faults at different systems. At the next step, possible faults intentionally and virtually are applied to the system, then like a normal state, the faulty system is diagnosed. Afterward, for each fault, one model like figure 1 is created that can be compared by system output with output model.

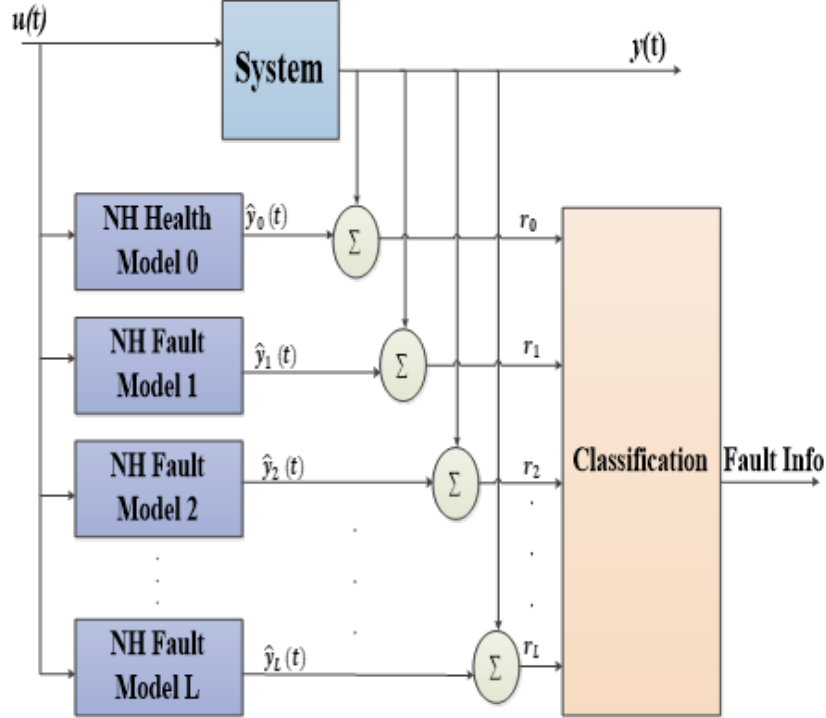


Figure 1: Proposed fault diagnosis model.

Create remains based on equation (1) then calcify faults:

$$r_i = y(t) - \hat{y}_i(t), \quad (1)$$

where, according to figure 1, system output $y(t)$ is contrasted to output model system without fault $\hat{y}_0(t)$ and output faulty model like $\hat{y}_1(t)$ to $\hat{y}_n(t)$, remained amounts (r_0 to r_n) according to relation (1) are created and for pattern recognition is categorized with neural network.

In sequence, at first, the electrical power system is simulated with neural networks without fault which is a powerful tool in system recognition [15], and then possible faults are injected into the system and then they are simulated and graph is given.

2.1 Electrical power system modeling

The electrical power system of the satellite is provided by a solar array with convert sun radiation power. Sun radiation power of solar array is influenced by environmental circumstances. Because of the array function and power system, both are influenced by the rate of solar radiation and solar cell surface temperature [14]. Solar array temperature is dependent on the environmental circumstance like the rate of sun radiation, thermal flux includes sun thermal flux, albedo thermal flux, and earth sub radiant flux. Solar array productive current is dependent on to rate of solar radiation directly. Therefore, two parameters, sun radiation power and solar array temperature that are directly affected to produce power and satellite power system are system inputs after simulating the power system in MATLAB software.

Nanosatellite has insufficient space, volume, and mass for installing sensors also for decreasing cost of project and satellite launch, for modeling power system is consumed that output load current as output and system according to

nonlinear properties as static nonlinear are based on equation (3).

$$I_{\text{load}} = f(P_{\text{sun}}, T), \quad (2)$$

where I_{load} is the load output current (A), P_{sun} is sun radiation power (e.g. W/m^2), and T is solar array temperature (Celsius degree). The electrical power system is consisting of elements and components. Model of each subsystem and create a link between these models is complicated and token a lot of time. Because of this reason for modeling the whole system, one can assume these parts as one part, their inputs and output are considered and the black box is identified by virtual neural networks.

For identifying system from tree layer virtual neural network, with the Marquardt algorithm [18], random data categorizing, elementary activated function, and tansig from mean squire variance of fault are used based on equation (4).

$$E = \frac{1}{n} \sum_{k=1}^n (y_k - \hat{y}_k)^2, \quad (3)$$

At equation (4), y_k is system output, \hat{y}_k is model output and n is data number. In addition to these, for analyzing neural network accurately is used network output coherent scale, system output and also studies its statistical behavior (average amount and fault variance) from fault graph histogram.

Modeling result is shown in Figure 2.

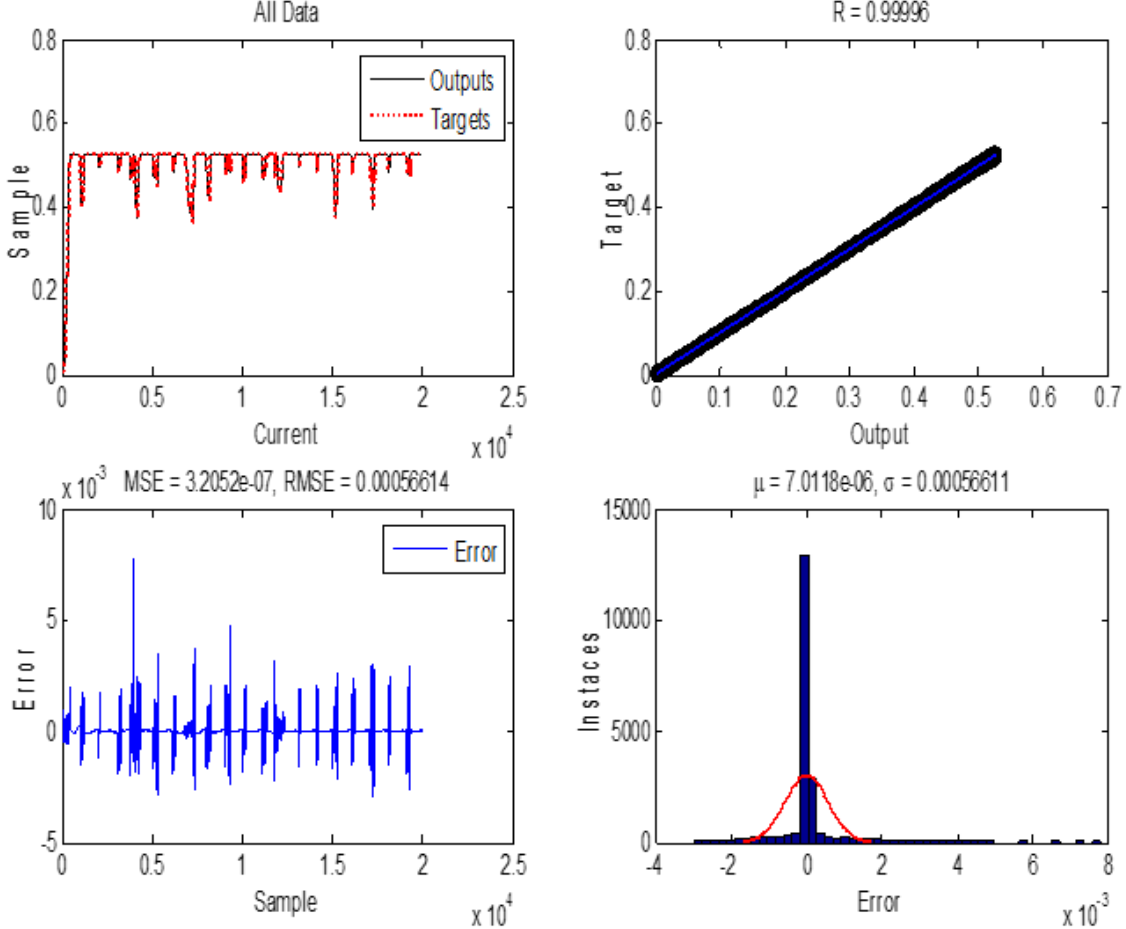


Figure 2: System output coherent and its estimated amount, the output electrical power system without fault and its estimated amount diagram, estimated fault histogram and amount of fault square average, and the average of fault square based on samples.

At MPPT converter for calculating power optimization photovoltaic subsystem use current and voltage sensors until to sampling this parameter instantly, that amount will compare with optimization amounts [19]. Because of this for

diagnosing and calcification possible faults at photovoltaic subsystem can use these sensors and from moving fault of a solar array at power system prevent and diagnose more quickly. For this reason, for modeling the photovoltaic subsystem as before inputs are sun radiation power and solar array surface temperature and outputs are current and voltage of arrays and with using of neural networks, nonlinear assumption and static, the system is identifying. The results are shown in Figures 3 and 4.

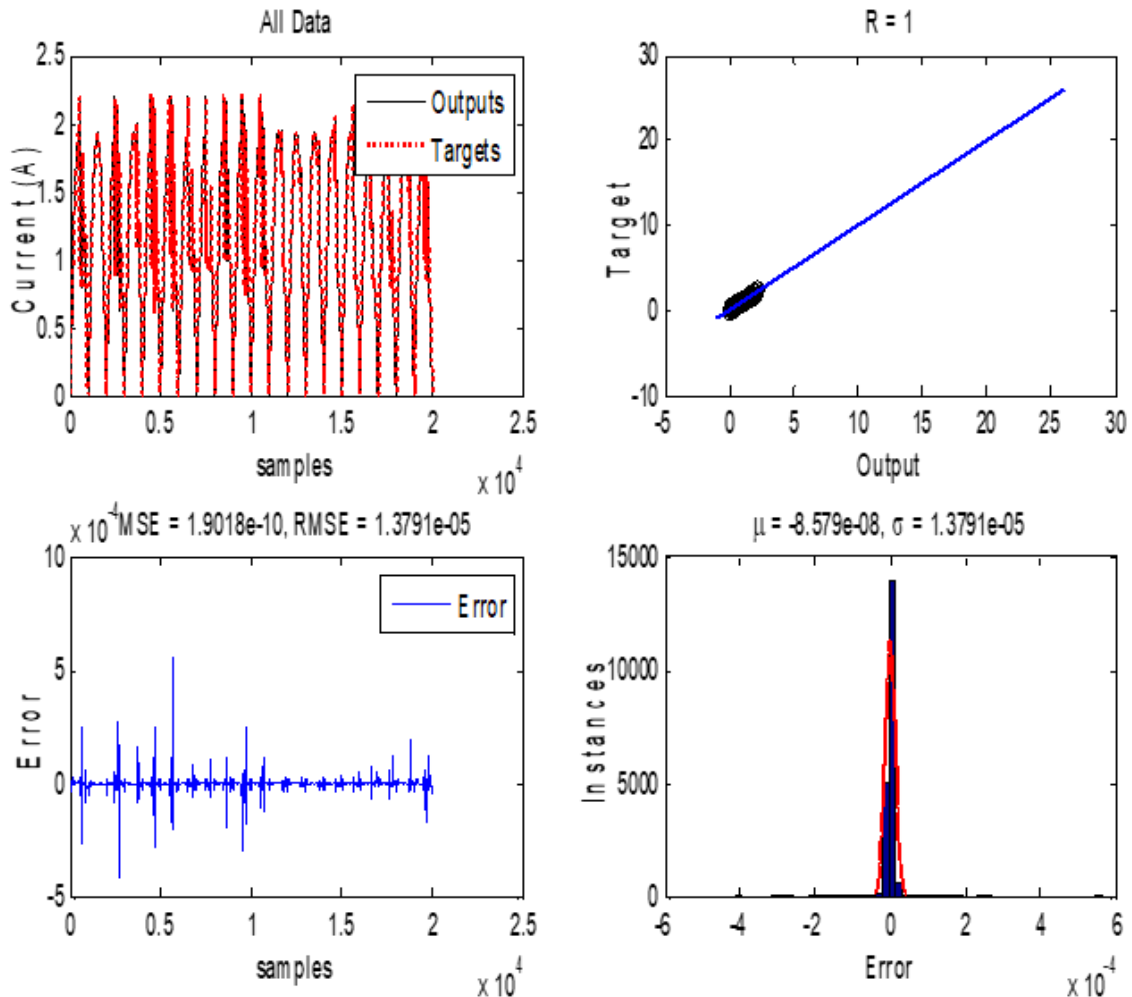


Figure 3: Current of photovoltaic system output coherent and its estimated amount, output diagram and its estimated amount, estimated fault histogram, and amount of fault square average and average of fault square based on samples.

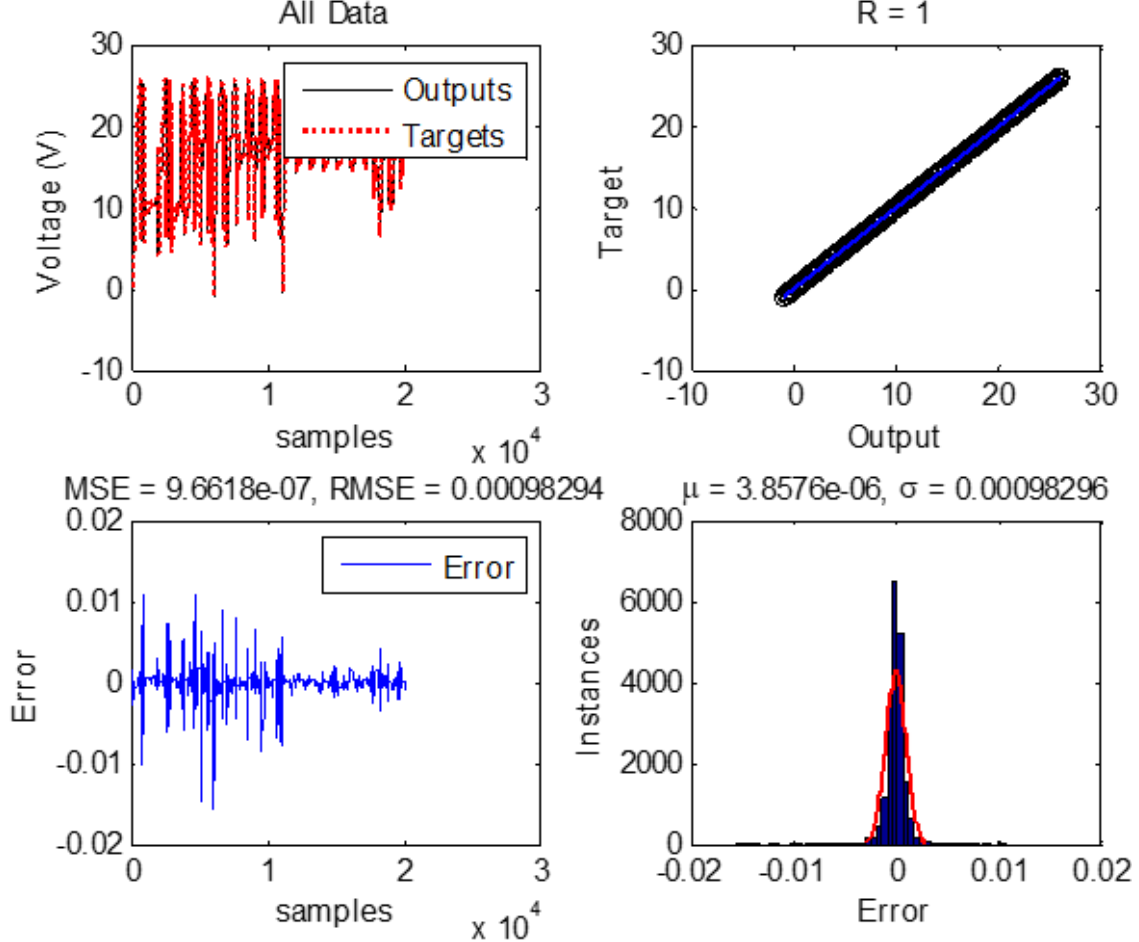


Figure 4: Voltage of photovoltaic system output coherent and its estimated amount, output diagram and its estimated amount, estimated fault histogram, and amount of fault square average and an average of fault square based on samples.

With a study on Figures 2 to 4 is observed that neural network have high accuracy for output model based on system output is estimated that is oscillating, real and estimate output similarity rate on the system modeling with current load is 96% and at photovoltaic system model is 100%. Fault on the modeling is considered parameters as the average of fault square, average and fault variance. At previous simulates, the amount of average square fault is less than 10^{-6} at system modeling with load current, at photovoltaic system outputs is less than 10^{-6} at the voltage and 10^{-9} at current. With a study on faults' histogram graph at Figures 2 to 4 is observed that faults' average at system modeling is less than 10^{-5} , photovoltaic system outputs are less than 10^{-6} at the voltage and 10^{-9} at current. The fault of variance at previous modeling as the sequence is 0.00056, 0.00013, and 0.00098. At faults' histogram is seen that the Gaussian estimate of modeling faults at Figures 2 to 4 are ideal at the peak that it is a symptom of faults that aren't separated from the average amount. As a result, above the neural network has suitable accuracy for the electrical power system model without fault.

2.2 Faulty electrical power system modeling

Faults happen as random at electrical and electronic systems [13]. With attention to this assumption, each possible fault must inject into the system and identify a system model with a neural network. As a sequence, open circuit and line-line fault at the solar array, MPPT converter IGBT open circuit fault, open circuit fault, short circuit IGBT regulator converter, and battery ground fault are identified based on section 2 and is summarized at Table 2.

Table 2: Summary of faulty electrical power system modeling results.

Subsystem	Fault model	System output coherent	RMSE	Fault average μ	Fault variance δ
Photovoltaic	Open circuit current	1	10^{-11}	3.6×10^{-7}	6.7×10^{-6}
	Open circuit voltage	1	10^{-5}	0.00225	0.00921
	Line-line current	0.99838	0.00056	0.00032	0.02375
	Line-line voltage	1	10^{-8}	10^{-6}	0.00103
IGBT MPPT	Open circuit load current	0.99999	10^{-8}	5.3×10^{-7}	0.00023
IGBT regulator converter	Open circuit load current	0.99963	10^{-10}	10^{-8}	9.5×10^{-5}
	Short circuit load current	0.99986	10^{-6}	10^{-6}	0.0122
Battery	Ground load current	1	10^{-8}	10^{-8}	0.00012

2.3 Photovoltaic subsystem faults calcification with neural network MLP

At the photovoltaic subsystem, possible faults are line-line and open circuit. For fault determining and calcification can also use neural network MLP. Healthy photovoltaic system model, line-line, and open circuit fault were calculated in the previous section. Now, the model output vector compare with the system output vector, amount remains are built based on equation (5) and as input enter to classifier.

$$r = [V_{\text{pv}} - \hat{V}_{\text{pv}}, I_{\text{pv}} - \hat{I}_{\text{pv}}], \quad (4)$$

At equation (5), r is the remaining amounts, V_{pv} and I_{pv} are the amounts of voltage and current are for the photovoltaic system, \hat{V}_{pv} and \hat{I}_{pv} are the amounts of output voltage and current of a photovoltaic system. The number of simulation data for the classifier is 2001 that which is provided for each class. The output is 3 bit that identifies faults classes. The result of this calcification is shown at the confusion matrix Figure 5.



Figure 5: Neural network classifier confusion matrix MLP for identifying fault of a photovoltaic system.

A study on Figure 5 is defined that neural network accuracy for classification of possible fault at photovoltaic system is more than 99.9% that explains its accuracy but calcification accuracy at model classes without fault as the sequence is line-line and open circuit. Also, it is clear that from 2001 model class data without fault 1998 data is classified correctly and 3 data have a fault, it means that the accuracy detects of this class is approximately 99.9%. In photovoltaic system class accuracy of fault is 99.3% from 2001 data, 1968 data are correct and 15 data are not correct that are calcified. Also in open circuit fault class accuracy is 98.5% from 2001 data, 1970 data is correct and 31 data is not correct that is detected. A study on Figure 5 also can see that from 3 data which are not correct and are diagnosed in system class without fault, 2 data are in line-line fault class and 1 data are in open circuit fault class that are classified incorrectly. Classification fault in line-line fault class from each 15 data is in open circuit fault class and from 31 data must be in open circuit fault class. 28 numeric data are in line-line fault class and 3 numeric data are in model class without fault.

2.4 Electrical power system fault classification with neural network MLP

For classification, another possible fault at the electrical power system from the neural network MLP tree layer with allocating 5 bit to 5 output class, consist of a system without fault, the battery is a ground fault, open circuit IGBT converter MPPT fault, open circuit fault, and short circuit IGBT regulate convertor. Inputs of neural clarification are based on figure 1 that are consists of neural models output and output amount of the system based on equation (6).

$$x = [r_0, r_1, \dots, r_4] \quad (5)$$

In equation (6), r_i are remain amounts and x is the input vector to neural classifier figure 1. With enter input of equation (6) to confusion matrix classifier, Figure 6 is gained.

		Confusion Matrix					
		1	2	3	4	5	
Output Class	1	1096 11.0%	0 0.0%	22 0.2%	12 0.1%	183 1.8%	83.5% 16.5%
	2	0 0.0%	1988 19.9%	0 0.0%	18 0.2%	0 0.0%	99.1% 0.9%
	3	457 4.6%	0 0.0%	1534 15.3%	3 0.0%	408 4.1%	63.9% 36.1%
	4	46 0.5%	0 0.0%	0 0.0%	1950 19.5%	9 0.1%	97.3% 2.7%
	5	402 4.0%	13 0.1%	445 4.4%	18 0.2%	1401 14.0%	61.5% 38.5%
		54.8% 45.2%	99.4% 0.6%	76.7% 23.3%	97.5% 2.5%	70.0% 30.0%	79.7% 20.3%

Figure 6: Confusion matrix neural network classifier MLP at the first state.

Figure 6 shows that neural network MLP can diagnose 1096 data from 2001 data at first-class and has 54.8% accuracy and 45% fault. As sequence 457, 46, and 402 are in open circuit fault IGBT converter MPPT, open circuit fault and short circuit IGBT regulate convertor. Classifier accuracy at ground battery fault class is more than other classes and is more than 99%, 13 data in IGBT short circuit fault class is incorrect. Rate of accuracy in the designed neural network at the separation between classes, MPPT converter open circuit fault, and open circuit fault and regulate convertor IGBT short circuit as sequent are 76.7%, 97.5%, and 70% it means that accuracy in separate IGBT open circuit fault regulator converter is good and was diagnosed incorrectly 12 data class without fault, 18 data at ground battery fault, 3 data at IGBT open circuit MPPT converter fault and 18 data at regulating convertor IGBT short circuit fault class. Finally, the confusion matrix is shown in Figure 6 which this neural network MLP at several states of Nanosatellite electrical power system has 79.7% accuracy and has 20.3% fault. Therefore, with these results and accuracies cannot use the network and its outputs for system faults classification.

For overcoming to insufficient accuracy of the neural network and increase accuracy can use from another feature of the output signal (load current). Adding the first Moment vector (current amount average for every moment) output current as one of the generated properties, based on equation (7) and (8) is identified.

$$m_1 = \frac{1}{N} \sum_{k=1}^N I_{\text{load}}(k) \quad (6)$$

In equations (7) and (8), m_1 is the first output current moment and r_i are remain amounts of neural models. With entering previous outputs to tree layer neural network MLP and study 2001 data at each class of confusion matrix, this classification was calculated according to Figure 7. Confusion matrix in Figure 7 is diagonal and shows that 100% of data are correctly categorized in fifth classes and designed neural network MLP could be detected all state of a faulty system with high accuracy because 20% of data, it means 2001 data is each class and classification fault in each class based on Figure 7 is zero.

		Confusion Matrix					
		1	2	3	4	5	6
Output Class	1	2001 20.0%	0 0.0%	0 0.0%	0 0.0%	0 0.0%	100% 0.0%
	2	0 0.0%	2001 20.0%	0 0.0%	0 0.0%	0 0.0%	100% 0.0%
	3	0 0.0%	0 0.0%	2001 20.0%	0 0.0%	0 0.0%	100% 0.0%
	4	0 0.0%	0 0.0%	0 0.0%	2001 20.0%	0 0.0%	100% 0.0%
	5	0 0.0%	0 0.0%	0 0.0%	0 0.0%	2001 20.0%	100% 0.0%
	6	100% 0.0%	100% 0.0%	100% 0.0%	100% 0.0%	100% 0.0%	100% 0.0%

Figure 7: Confusion matrix neural network MLP classification with 5 bits' output.

2.5 Fault classification with another intelligence method

Calculate the average amount of output load current at each moment may impose a heavy calculating load to the system processor, for this reason, can use another intelligence method for separating system faults.

In the satellite electronics power system for controlling and managing battery charge and de charge use SOC parameter with battery charge state. A precision estimate of the battery charge state protects from battery health, unnecessary charge, and de charge of the battery increases the life of the battery, decreases the probability of happening fault, and increases system reliability [9]. SOC parameter is calculated by Kalman. With the use method [20] SOC was calculated. Now with use intelligence classification methods like PCA, KNN, and decision tree can proceed to possible fault classification of power system with current load inputs and battery SOC.

2.5.1 KNN method

For fault classification also can use the KNN method. KNN is a lazy classifier and data is classifying without build model and learning samples. With the use KNN classifier method and with use output current inputs, battery charge state and build Ordered pair (I_{load} , SOC) are defined possible fault in satellite electrical power, K is geometric distance Euclidean based on equation (9), around each Ordered pair (I_{load} , SOC) is used for data classification [21].

$$d = \sqrt{(I_{load} - I_k)^2 + (\text{SOC} - \text{SOC}_k)^2} \quad (7)$$

In the above equation d is the geometric distance, I_{load} is loaded current and (I_k, SOC_k) is point k charge state in the plane of figure (7). For evaluating the function at this algorithm can proceed to study on cross-validation and Resubstituting Loss parameters. In cross-evaluation, data is separated into K group, and then learning operation and cross-test on each group, K-fold Loss parameter is defined.

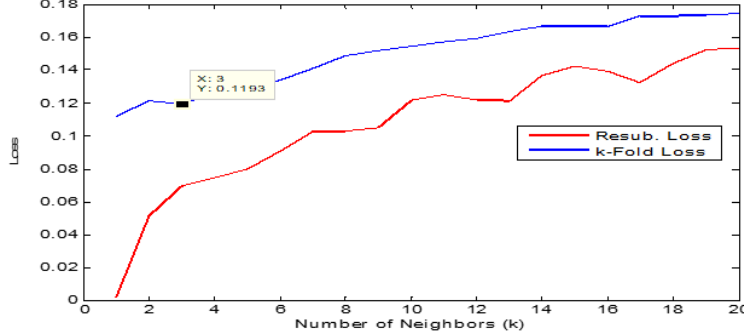


Figure 8: K-Fold faults and replacement at KNN method.

With a study on figure 8 is determined that number of neighbors in the KNN method must choose equivalent 3 with Resubstituting Loss and K-Fold Loss because Resubstituting Loss fault one or two near neighbor is down but choose K parameter equivalent 1 and 2 cause classifier over coherency to data learning. To determine the number of neighbors, fault classification is done and is presented at Table 3.

$$\text{Resubstitution Loss} \approx 0.0698 \sim 7\%, \quad \text{K_Fold Loss} \approx 0.1193 \sim 12\%$$

Table 3: Result of KNN classification method.

Class	Accuracy (%)	Notes
System without fault	86	
Battery ground fault	100	
Open circuit IGBT MPPT	86	
Open circuit regulator	99.99	
Short circuit IGBT regulator	92	

At the table (3) is observing that the KNN algorithm cannot classify fault completely.

2.5.2 Decision tree

For separate and apart existence classes can use a learning tree or decision tree. Decision tree is the method for estimating objective with discrete amounts. This method is one of the most famous of a posteriori learning algorithms that use in the different application successfully and this method has resistance to input data noise. Decision tree learning is using the ID3 algorithm. Based on decision tree calcification is choosing a strategy that has the most likelihood [21].

For separating system with or without fault from the decision tree method is using output load current and battery charge state such as PCA and KNN methods, table (4) is presenting fault calcification result, replacement fault rate and k replicate.

$$\text{Resubstituting Loss} \approx 0.0137 \sim 1.3\%, \quad \text{K_Fold Loss} \approx 0.0435 \sim 4.3\%$$

Table 4: Decision tree classification result.

Class	Accuracy (%)	Notes
System without fault	97	
Battery ground fault	99.99	
Open circuit IGBT MPPT	98	
Open circuit regulator	99.6	
Short circuit IGBT regulator	98.35	

2.5.3 PCA method

PCA method is a linear mapping between inputs and outputs that the discrete system is based on their Eigenvalue and Eigenvector. Figure 9 is presenting inputs the plane of output load current and battery charge state at system fault class and possible species fault sin system at two dimensions, before act PCA method.

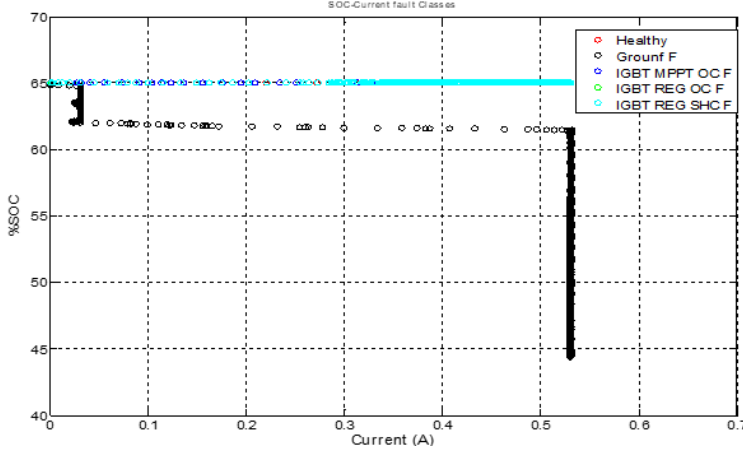


Figure 9: Fault species on the plane of battery charge state and load current.

Figure 8 is presenting tat states of without faults and possible fault classes on the electrical power system at two dimensions' plane of battery charge state and output load current cannot discrete.

For using the PCA method, first of all, inputs classifiers are Ordered pair (I_{load} , SOC) and matrix X at equation (9) is considered.

$$X = \begin{bmatrix} I_{\text{load},1} & \cdots & I_{\text{load},N} \\ \text{SOC}_1 & \cdots & \text{SOC}_N \end{bmatrix}$$

Also in equation (9), y is mapping output vector and Q is the Eigenvector matrix for covariance matrix C in equation (10). At this equation average data (bias) is equal zero, defined as below:

$$C = \frac{1}{N} X X^\top$$

For calculating the equation of the PCA method, matrix Q , Eigenvector for the biggest Eigenvalue Matrix C is determined ascending in the column of matrix Q and then choose Eigenvectors that have bigger Eigenvalue as a result produce more variance dispersion in y output. Separation and calcification result fault with the PCA method is without fault state and fault class species are presented in Figure 10.

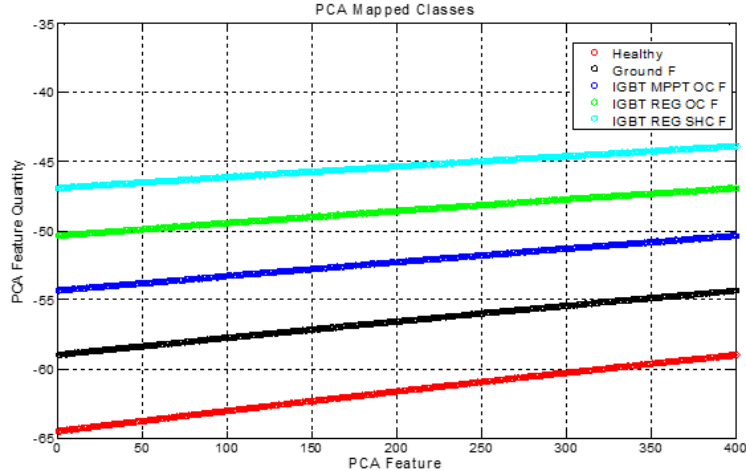


Figure 10: Separating possible fault in the electrical power system with the PCA method.

Figure 10 is proposing that without fault and possible fault species are reduced to one dimension and with suitable space and are separated by the PCA method.

The result for the conclusion presented methods of separating faults at the electrical power system except for photovoltaic subsystems is brought at the Table 5.

Table 5: Compare classification methods for electrical power system faults.

Method	System	Accuracy (%)
Neural network (MLP)	Electrical power	100
	Photovoltaic	99.2
PCA	Electrical power	100
KNN	Electrical power	93
DT	Electrical power	98.6

Table (5) depicts that the accuracy of neural network MLP and PCA method which are two algorithms for separate and classification possible fault in the electrical power system of Nanosatellite is more than others. DT method also had high accuracy but the KNN method based on its accuracy cannot use for this purpose. For analysis quality of classification possible fault in the electrical power system in each class, can refer to Table 7 (omitted here for brevity).

3 Conclusion

This paper is a proposed simulation of the satellite electrical power system in Nanosatellite. Effective parameters on the function of a power system are inputs and the electrical load current is output because of mass and volume limitation and with consideration to these parameters and use reliability analysis of neural network on system equipment, electrical system model without fault state and with possible fault was determined with suitable accuracy. Then were used classification neural network MLP, PCA, KNN, and DT methods for separating classes and presented that neural network MLP and PCA method can separate and classify without fault system and possible fault classes and were more effective than KNN and DT methods.

References

- [1] M. Patel. *Spacecraft power systems*. CRC Press, 2004.
- [2] J. Gonzalez-Llorente and E. Ortiz-Rivera. Comparison of Maximum Power Point Tracking Techniques in Electrical Power Systems of CubeSat. Conference on Small Satellites, 2013.
- [3] Y. Zhao et al. Graph-based semi-supervised learning for fault detection and classification in solar photovoltaic arrays. *IEEE Transactions on Power Electronics*, 30(5):2848–2858, 2015.
- [4] Y. Zhao et al. Decision tree-based fault detection and classification in solar photovoltaic arrays. In *Twenty-Seventh Annual IEEE Applied Power Electronics Conference and Exposition (APEC)*, 2012.
- [5] A. H. Mohamed and A. M. Nassar. New Algorithm for Fault Diagnosis of Photovoltaic Energy Systems. *International Journal of Computer Applications*, 114(9), 2015.
- [6] N. M. A. Freire, J. O. Estima, and A. J. M. Cardoso. A voltage-based approach without extra hardware for open-circuit fault diagnosis in closed-loop PWM AC regenerative drives. *IEEE Transactions on Industrial Electronics*, 61(9):4960–4970, 2014.
- [7] Y. He et al. A new model for State-of-Charge (SOC) estimation for high-power Li-ion batteries. *Applied Energy*, 101:808–814, 2013.
- [8] S. Sepasi, R. Ghorbani, and B. Y. Liaw. A novel on-board state-of-charge estimation method for aged Li-ion batteries based on model adaptive extended Kalman filter. *Journal of Power Sources*, 245:337–344, 2014.
- [9] A. Nuhic et al. Health diagnosis and remaining useful life prognostics of lithium-ion batteries using data-driven methods. *Journal of Power Sources*, 239:680–688, 2013.
- [10] B. Lee and X. Wang. Fault detection and reconstruction for micro-satellite power subsystem based on PCA. In *Systems and Control in Aeronautics and Astronautics (ISSCAA)*, 2010 3rd International Symposium on. IEEE, 2010.

- [11] S. Xie et al. Fault diagnosis of the satellite power system based on the Bayesian network. In *Computer Science & Education (ICCSE)*, 2013 8th International Conference on. IEEE, 2013.
- [12] T. T. Wong. A hybrid discretization method for naïve Bayesian classifiers. *Pattern Recognition*, 45(6):2321–2325, 2012.
- [13] R. Isermann. Fault-diagnosis systems: an introduction from fault detection to fault tolerance. Springer, 2006.
- [14] M. Vázquez and I. Rey-Stolle. Photovoltaic module reliability model based on field degradation studies. *Progress in Photovoltaics: Research and Applications*, 16(5):419–433, 2008.
- [15] R. J. Patton and J. Chen. A review of parity space approach to fault diagnosis. In *IFAC Safeprocess Conference*, 1991.
- [16] S. Chen, S. A. Billings, and P. M. Grant. Non-linear system identification using neural networks. *International Journal of Control*, 51(6):1191–1214, 1990.
- [17] L. Jacques. Thermal design of the oufti-1 nanosatellite. PhD thesis, University of Liège, 2009.
- [18] M. T. Hagan and M. B. Menhaj. Training feedforward networks with the Marquardt algorithm. *IEEE Transactions on Neural Networks*, 5(6):989–993, 1994.
- [19] B. Subudhi and R. Pradhan. A comparative study on maximum power point tracking techniques for photovoltaic power systems. *IEEE Transactions on Sustainable Energy*, 4(1):89–98, 2013.
- [20] W. He et al. State of charge estimation for Li-ion batteries using neural network modeling and unscented Kalman filter-based error cancellation. *International Journal of Electrical Power & Energy Systems*, 62:783–791, 2014.
- [21] S. R. Gaddam, V. V. Phoha, and K. S. Balagani. K-Means+ID3: A novel method for supervised anomaly detection by cascading K-Means clustering and ID3 decision tree learning methods. *IEEE Transactions on Knowledge and Data Engineering*, 19(3):345–354, 2007.
- [22] S. Abdoli and F. Hajati, Offline signature verification using geodesic derivative pattern, in 2014 22nd Iranian Conference on Electrical Engineering (ICEE), 2014: IEEE, pp. 1018–1023.
- [23] F. Ayatollahi, A. A. Raie, and F. Hajati, Expression-invariant face recognition using depth and intensity dual-tree complex wavelet transform features, *Journal of Electronic Imaging*, vol. 24, no. 2, pp. 023031-023031, 2015.
- [24] L. Barolli, Advanced Information Networking and Applications: Proceedings of the 38th International Conference on Advanced Information Networking and Applications (AINA-2024), Volume 2, ed: Springer Nature, 2024.
- [25] L. Barolli, P. Hellinckx, and T. Enokido, Advances on Broad-Band Wireless Computing, Communication and Applications: Proceedings of the 14th International Conference on Broad-Band Wireless Computing, Communication and Applications (BWCCA-2019). Springer Nature, 2019.
- [26] L. Barolli, M. Takizawa, F. Xhafa, and T. Enokido, Web, Artificial Intelligence and Network Applications: Proceedings of the Workshops of the 33rd International Conference on Advanced Information Networking and Applications (WAINA-2019). Springer, 2019.
- [27] R. Barzamini, F. Hajati, S. Gheisari, and M. Motamadinejad, Short term load forecasting using multi-layer perception and fuzzy inference systems, *Journal of Applied Sciences*, vol. 12, no. 1, pp. 40-47, 2012.
- [28] D. Cremers, I. Reid, H. Saito, and M.-H. Yang, Computer Vision–ACCV 2014: 12th Asian Conference on Computer Vision, Singapore, Singapore, November 1-5, 2014, Revised Selected Papers, Part V. Springer, 2015.
- [29] S. Fiorini, F. Hajati, A. Barla, and F. Girosi, Predicting diabetes second-line therapy initiation in the Australian population via timespan-guided neural attention network, *PLOS ONE*, vol. 10, no. 14, p. e0211844, 2019.
- [30] F. Hajati, A. Cheraghian, S. Gheisari, Y. Gao, and A. S. Mian, Surface geodesic pattern for 3D deformable texture matching, *Pattern Recognition*, vol. 62, pp. 21-32, 2017.
- [31] F. Hajati, K. Faez, and S. K. Pakazad, An Efficient Method for Face Localization and Recognition in Color Images, in *Systems, Man and Cybernetics, 2006. SMC’06. IEEE International Conference on*, 2006, vol. 5: IEEE, pp. 4214-4219.
- [32] F. Hajati, A. A. Raie, and Y. Gao, Pose-invariant 2.5 D face recognition using geodesic texture warping, in 2010 11th International Conference on Control Automation Robotics & Vision, 2010: IEEE, pp. 1837-1841.
- [33] F. Hajati, M. Tavakolian, S. Gheisari, Y. Gao, and A. S. Mian, Dynamic texture comparison using derivative sparse representation: Application to video-based face recognition, *IEEE Transactions on Human-Machine Systems*, vol. 47, no. 6, pp. 970-982, 2017.

[34] P. Mahajan, S. Uddin, F. Hajati, M. A. Moni, and E. Gide, A comparative evaluation of machine learning ensemble approaches for disease prediction using multiple datasets, *Health and Technology*, vol. 14, no. 3, pp. 597-613, 2024.

[35] S. K. Pakazad, K. Faez, and F. Hajati, Face Detection Based on Central Geometrical Moments of Face Components, in *Systems, Man and Cybernetics, 2006. SMC'06. IEEE International Conference on*, 2006, pp. 4225-4230.

[36] A. Sadeghi, M. Sadeghi, A. Sharifpour, M. Fakhar, Z. Zakariaei, and F. Hajati, Potential diagnostic application of a novel deep learning-based approach for COVID-19, *Nature Scientific Reports*, vol. 14, no. 1, p. 280, 2024.

[37] F. Shojaiee and F. Hajati, Local composition derivative pattern for palmprint recognition, in *2014 22nd Iranian Conference on Electrical Engineering (ICEE)*, 2014: IEEE, pp. 965-970.

[38] C. J. P. Sopo, F. Hajati, and S. Gheisari, DeFungi: Direct mycological examination of microscopic fungi images, *arXiv preprint arXiv:2109.07322*, 2021.

[39] A. Tavakolian, F. Hajati, A. Rezaee, A. O. Fasakhodi, and S. Uddin, Fast COVID-19 versus H1N1 screening using optimized parallel inception, *Expert systems with applications*, vol. 204, p. 117551, 2022.

[40] A. Tavakolian, A. Rezaee, F. Hajati, and S. Uddin, Hospital readmission and length-of-stay prediction using an optimized hybrid deep model, *Future Internet*, vol. 15, no. 9, p. 304, 2023.

[41] S. Wang, H. Lu, A. Khan, F. Hajati, M. Khushi, and S. Uddin, A machine learning software tool for multiclass classification, *Software Impacts*, vol. 13, p. 100383, 2022.

[42] M. Karimi and A. Rezaee, Regularization of the Cauchy problem for the Helmholtz equation by using Meyer wavelet, *Journal of Computational and Applied Mathematics*, vol. 320, pp. 76-95, 2017.

[43] B. Mohamadzade and A. Rezaee, Compact and broadband dual sleeve monopole antenna for GSM, WiMAX and WLAN application, *Microwave and Optical Technology Letters*, vol. 59, no. 6, pp. 1271-1277, 2017.

[44] M. Ramezani, M. Amiri Atashgah, and A. Rezaee, A Fault-Tolerant Multi-Agent Reinforcement Learning Framework for Unmanned Aerial Vehicles–Unmanned Ground Vehicle Coverage Path Planning, *Drones*, vol. 8, no. 10, p. 537, 2024.

[45] A. Rezaee, Genetic symbiosis algorithm generating test data for constraint automata, *Applied and Computational Mathematics*, vol. 6, no. 1, pp. 126-137, 2008.

[46] A. Rezaee, Using Genetic Algorithms for Designing of FIR Digital Filters, *ICTACT journal on Soft computing*, vol. 1, no. 1, pp. 18-22, 2010.

[47] A. Rezaee, Determining PID controller coefficients for the moving motor of a welder robot using fuzzy logic, *Automatic Control and Computer Sciences*, vol. 51, no. 2, pp. 124-132, 2017.

[48] A. Rezaee, DESIGN, CONSTRUCTION AND EVALUATION OF A DIGITAL HAND-PUSHED PENETROMETER, *International Journal of Advanced Smart Sensor Network Systems*, vol. 7, no. 1, pp. 1-10, 2017.

[49] A. Rezaee, Model predictive for Mobile robot control, *Transactions on environment and electrical engineering*, vol. 2, no. 2, pp. 17-22, 2017.

[50] A. Rezaee and M. K. Golpayegani, Intelligent Control of Cooling-Heating Systems by Using Emotional Learning, *Electronics and electrical engineering*, vol. 18, no. 4, pp. 26-30, 2012.

[51] A. Rezaee and M. Pajohesh, Suspension system control with fuzzy logic, *Journal of Communications Technology, Electronics and Computer Science*, vol. 6, pp. 1-5, 2016.

[52] A. Sadeghi, F. Hajati, A. Rezaee, M. Sadeghi, A. Argha, and H. Alinejad-Rokny, 3DECG-Net: ECG fusion network for multi-label cardiac arrhythmia detection, *Computers in Biology and Medicine*, vol. 182, p. 109126, 2024.

[53] H. Taghvaei, S. M. Seyyedi, and A. Rezaee, Design of Metamaterial Dual Band Absorber, in *The third Iranian Conference on Engineering Electromagnetic*, 2014.

[54] A. Tavakolian, F. Hajati, A. Rezaee, A. O. Fasakhodi, and S. Uddin, Source code for optimized parallel inception: A fast COVID-19 screening software, *Software Impacts*, vol. 13, p. 100337, 2022.

[55] E. Gavagsaz, A. Rezaee, and H. Haj Seyyed Javadi, Load balancing in reducers for skewed data in MapReduce systems by using scalable simple random sampling, *The Journal of Supercomputing*, vol. 74, no. 7, pp. 3415-3440, 2018.

[56] A. Rezaee, A. M. Rahmani, A. Movaghar, and M. Teshnehlab, Formal process algebraic modeling, verification, and analysis of an abstract Fuzzy Inference Cloud Service, *The Journal of Supercomputing*, vol. 67, no. 2, pp. 345-383, 2014.

- [57] S. Sarvghad, A. Rezaee, and F. Masomi, On the Relationship between Thinking Styles and Self-Efficacy of Pre-University Students in Shiraz, 2011.
- [58] I. Shahramian, E. Akhlaghi, A. Ramezani, A. Rezaee, N. Noori, and E. Sharafi, A study of leptin serum concentrations in patients with major beta-thalassemia, Iranian journal of pediatric hematology and oncology, vol. 3, no. 2, p. 59, 2013.
- [59] I. Shahramian, M. Razzaghian, A. A. Ramazani, G. A. Ahmadi, N. M. Noori, and A. R. Rezaee, The correlation between troponin and ferritin serum levels in the patients with major beta-thalassemia, International cardiovascular research journal, vol. 7, no. 2, p. 51, 2013.